JCTC Journal of Chemical Theory and Computation

Article

pubs.acs.org/JCTC

BALOO: A Fast and Versatile Code for Accurate Multireference Variational/Perturbative Calculations

Ivo Cacelli,*[,†,‡] Alessandro Ferretti,[‡] Giacomo Prampolini,[‡] and Vincenzo Barone[§]

[†]Dipartimento di Chimica e Chimica Industriale, Università di Pisa, Via Moruzzi 3, I-56124 Pisa, Pisa, Italy

[‡]Istituto di Chimica dei Composti OrganoMetallici (ICCOM-CNR), Area della Ricerca, via G. Moruzzi 1, I-56124 Pisa, Pisa, Italy

[§]Scuola Normale Superiore, Piazza dei Cavalieri 7, I-56125 Pisa, Pisa, Italy

Supporting Information

ABSTRACT: We present the new BALOO package for performing multireference variational/perturbative computations for medium- to large-size systems. To this end we have introduced a number of conceptual and technical improvements including full parallelization of the code, use and manipulation of a large panel of reference orbitals, implementation of diagrammatic perturbation treatment, and computation of properties by density matrix perturbed to the first-order. A number of test cases are analyzed with special reference to electronic transitions and magnetic properties to show the versatility, effectiveness, and accuracy of BALOO.

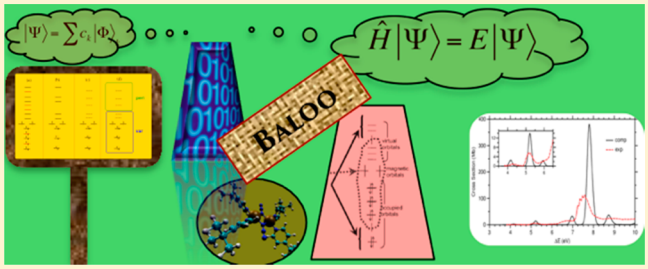

INTRODUCTION

The development of accurate yet effective methods for treating medium- to large-dimension systems involving large (static) correlation effects (hereafter broadly referred to as multireference systems) is still an important challenge of theoretical and computational chemistry. As a matter of fact, for molecular systems where a single reference description is a reasonable first approximation the coupled cluster singles-doubles with perturbative triples [CCSD(T)][1] approach is considered the golden standard of quantum chemistry and actually delivers remarkably accurate results when coupled with sufficiently large basis sets.[2] Ongoing attempts to improve the scaling of CCSD(T) with the number of active electrons together with developments of companion treatments (EOM-CCSD, etc.) for excited states, dominated by single excitations from a single reference ground state,[3] have great promise for these situations. At the same time, impressive advances of methods rooted in the density functional theory (DFT) and its time dependent extension (TD-DFT)[4] are paving an alternative route for reliable descriptions of even larger systems. However, the situation is different for true multireference cases, where the key to an accurate and conceptually satisfactory description is found behind the single-reference description and taking into account the multiconfiguration character from the very beginning.[5−8]

In nearly all cases, such electronic structure approaches can be divided into two steps. First, a qualitatively correct multi reference (MR) wave function is built, able to take into account the leading static correlation. This can be done in several ways, the conventional one resorting to a complete active space self-consistent field (CASSCF) wave function, in which a limited number of valence electrons is distributed in all possible ways over a set of valence orbitals. There are a number of advantages in this reference wave function, namely that it (i) can treat near-degeneracies, (ii) is a spin eigenfunction, and (iii) also provides a reasonable starting point when spin−orbit coupling becomes important.[9] However, full CASSCF can become prohibitive for large numbers of active electrons, and different strategies have been proposed in the literature that allow the use of incomplete reference spaces.[10]

The MR wave function can be improved by perturbation theory (MR-PT),[11] configuration interaction (MR-CI),[12,13] and coupled-cluster (MR-CC) approaches.[14] The best solution should be in principle offered by the MR-CC model, but, despite the quite large number of implementations proposed until now, a generally applicable method to tackle medium-size systems has not yet emerged. MR-CI has a long-standing tradition and is rather accurate but is plagued by the problems of lack of size-consistency and high computational cost. MR-PT is by far the most applied strategy, and the CASPT2 variant[15,16] has become a very popular working horse of wave function based quantum chemistry. However, also this approach has its own limitations, and we thought it interesting to develop a general MR-PT engine, whose MR part is as flexible as possible and whose PT part is made as efficient as possible thanks to a mixing of technical and methodological improvements. Before proceeding, let us mention two quite recent approaches along related lines. The first one is the NEVPT2 model by Cimiraglia and Angeli,[17,18] which has a number of appealing features, but still requires a full CASSCF reference wave function. The second method is the SORCI approach by Neese[19,20] where the whole electron space is divided into different subspaces, which

Received: November 28, 2014

DOI: 10.1021/ct501071k
J. Chem. Theory Comput. XXXX, XXX, XXX−XXX

are treated at different levels of approximation. Our Baloo code follows a philosophy quite similar to SORCI but introduces a number of distinctive features including full parallelization of the most demanding computational steps, optimization of the integral transformation, effective diagrammatic perturbative treatment, and computation of properties by the one-body density matrix perturbed to the first order, just to mention a few.

The paper is organized as follows. The next section contains a description of the main features of the new Baloo program following the logical steps of a full computation. Next we present a number of case studies with special reference to excitation energies and magnetic properties. Some conclusions and perspectives are provided in the last section.

THEORETICAL BACKGROUND AND TECHNICAL ASPECTS

Overview. BALOO ("the sleepy brown bear" in *The Jungle Book* by R. Kipling) is a program written in FORTRAN 95 to perform extended variational Configuration Interaction (CI) supplemented by Multi Reference (MR) perturbative calculations. The BALOO code proceeds from the old CIPSI program[21] and its successive improvements.[22,23] The original code has been totally rewritten in order to optimize its performances, simplify and generalize input data, exploit new possibilities offered by the FORTRAN 95 language, and parallelize all the critical parts of the calculation. Broadly speaking, BALOO was devised to allow for high level and accurate calculations of a number of molecular properties like excitation energies and general one-electron observables for both ground and excited states. To this end, several new computational strategies have also been implemented within the code.

A key feature of BALOO is the possibility of performing a sequence of CI calculations by gradually enlarging the configurational space according to some criteria usually based on MR perturbation theory (PT). This has the advantage of avoiding the *a priori* choice of the wave function restrictions expressed in terms of constraints on orbital occupancy, as instead necessary in CAS,[24] RAS,[25,26] ORMAS,[27] and similar methods. Thus, the extension of the many-electron basis set is completely automated, and, as detailed below, it can be driven by the property of interest. One of the main features of BALOO is the MR diagrammatic perturbation first proposed by Cimiraglia,[28] which has been proved to speed up dramatically the calculation and allows the user to consider perturbative spaces otherwise impractical.

In the following, the definition of the key ingredients and the different steps possibly involved in a BALOO calculation are described in detail.

One-Electron Basis Sets. The basic requirement for a BALOO calculation is a set of orthonormal molecular orbitals (MOs), which may come from any source like SCF, MC-SCF, or even DFT calculations. Furthermore, the working MOs may also be the Natural Orbitals of a previous BALOO calculation or the MOs coming from a Quantum Chemistry calculation and subsequently manipulated by the "in house" software QUIOLA,[29] which interfaces between the HF-like calculation and the four index transformation from atomic to molecular basis set. QUIOLA is able to localize onto specific fragments, diagonalizing the virtual (or occupied) MO block in a given one-electron potential and rearrange the sequence in order to facilitate the choice of the active MO space in the BALOO program (see below).

Four-Index Transformations. Once a set of MOs has been chosen, all the required one- and two-electron integrals are transformed from atomic to molecular basis set. This is performed by the IJKL program, originally included in the CIPSI package[21] but largely modified in the current version. For noncanonical MOs, IJKL also computes a double occupation Fock like matrix to be used by BALOO for the evaluation of the Hamiltonian matrix elements in the many electron basis set. The program has been efficiently parallelized exploiting the large RAM currently equipping modern High Performance computers. This implementation makes this step practically insignificant in comparison with the total cost of the full calculation.

Molecular Orbitals Partition and Configuration Definition. As usual, the one-electron basis set is partitioned into three different classes:

a) frozen MOs, i.e. orbitals that are doubly occupied in all configurations and not considered in four index transformation. BALOO only uses this set of MOs for the calculation of the required reduced density matrices in order to evaluate one-electron properties.

b) active MOs. These orbitals may have any occupation number in the variational space and are also considered in the intermediate perturbative steps, used to enlarge the variational space. This space will be also named Perturbative Active Space (PAS) as the included MOs are used in the perturbative approach at every step. The MO space used to build the many-electron variational space will be called Variational Active Space (VAS), and it is obviously a subspace of the PAS.

c) inactive MOs, which are silent during the BALOO sequence except in the final step, in the case Complementary Space Perturbative Approach (CSPA) or diagrammatic calculations (*vide infra*), are performed. Therefore, inactive MOs are doubly occupied or empty in all BALOO steps, and they are usually located at the beginning (doubly occupied) and/or at the end (empty) of the MO sequence.

Notice that the MO active space can be increased along the CI+PT2 steps in order to prepare more and more accurate CI wave functions to be used for the final perturbative step.

The many-electron space can be built with Configuration Spin Functions (CSF) as well as with Slater Determinants (SD). As is well-known, the CSFs are eigenvalues of the Spin operators and thus give rise to a much smaller space than SDs. Yet, in the cases where states with different spin are to be computed, the use of SDs can still be computationally convenient (e.g., for the singlet−triplet energy gap in diradicals). As the term "configuration" is used in a variety of contexts and sometimes with slightly different meanings, for the sake of clarity we define as Occupation Number Configurations (ONC) a sequence of occupation numbers 0,1,2 referred to as spatial orbitals. For instance in the case of the LiH molecule an ONC might be $(1\sigma)^2(2\sigma)^0(3\sigma)^1(4\sigma)^1$. In the framework of CSFs, once the spin symmetry has been defined, each ONC can be used to generate a number of CSFs, obtained from a linear combination of the SDs that have the desired spin value along the quantization z axis. Conversely, if SDs are used as a many-electron basis set, this *a priori* linear combination is not needed, and the spin symmetry of the wave function is made through suitable *a posteriori* linear combination of those SDs arising from the same ONC.

DOI: 10.1021/ct501071k
J. Chem. Theory Comput. XXXX, XXX, XXX−XXX

Storing Strategy and Matrix Element Evaluation. To efficiently exploit computer memory and to reduce hard disk occupancy, BALOO does not necessarily store all two-electron integrals read from the IJKL output file but only those really needed for the current type of calculation. For instance a CI calculation requires only those integrals with all indices in the VAS, whereas the subsequent MR perturbative calculation that uses CI states as zero-order wave function requires the addition of two-electron integrals having two indices in the PAS-VAS space, i.e. in the MO space active for perturbative calculations but not used in the current CI calculation. Exploiting these strategies, the available memory on last-generation computational resources can routinely handle up to 400−500 MOs in the active space.

The one- and two-electron matrix elements between CSFs (or SDs) are computed by implementing in an efficient way the formula tape method. The formulas are computed in a symbolic way as needed and then stored once for all. At the same time each type of matrix element is encoded in a single binary number, and all these numbers are arranged in increasing order, so that the searching procedure can be performed with the bisection method. By this algorithm, no more than 20 computer operations are sufficient to detect the right symbolic formula. The large memory requested for high excitation levels is not a serious problem, as when the memory devoted to the formula is filled, the program removes the stored data and resets the memory to store new formulas. The only limit in the many-electron basis set concerns the maximum excitation level, which in the present code has been fixed to 12, although there is no severe obstacle for further increasing. As discussed in more detail in the following, this and other new implementations make BALOO more than 100 times faster than more conventional (e.g., the old CIPSI) codes, without exploiting parallelization. Finally, calculations can be performed on neutral closed shell molecules as well as on positive and negative ions.

Variational CI Step. Once a variational space is assigned, an approximate time independent Schrödinger equation can be solved. This implies the solution of the CI eigenvalue problem projected in the variational space $\{V\}$ formed by the many-electron basis set

$$PHP|\Psi_K^{(0)}\rangle = E_K^{(0)}|\Psi_K^{(0)}\rangle \tag{1}$$

where $P = \sum_i^{\{V\}}|\Phi_i\rangle\langle\Phi_i|$ is the projector operator in the given space $\{V\}$ formed by the Slater determinants or CSFs Φ_i. Therefore, the CI states are expressed as

$$|\Psi_K^{(0)}\rangle = \sum_i^{\{V\}} C_{iK}^{(0)}|\Phi_i\rangle \tag{2}$$

Such eigenstates represent the variational approximation of the true eigenstates, and in view of the perturbative step, they will be also called zero-order states. Similarly, the variational eigenvalues are also called zero-order energies.

The evaluation of the lowest Hamiltonian eigensolutions is performed with the Davidson algorithm,[30] using also some additional expedients in order to improve the convergence and to restart the calculation in possible critical cases, e.g. when multiple eigenvalue flips may occur. Both disk-based and direct methods are implemented, although the latter approach becomes mandatory for large CI matrices. This step has been completely parallelized with an overall efficiency of about 80%.

Perturbative Step. The standard perturbative step (i.e., without exploiting diagrammatic techniques) following the variational CI calculation is a Rayleigh−Schrödinger first-order perturbative correction of the zero-order states

$$|\Psi_K^{(1)}\rangle = \sum_a^{\{\mathrm{FOIS}\}} \frac{\langle\Psi_K^{(0)}|H'|\Phi_a\rangle}{\varepsilon_K - \varepsilon_a}|\Phi_a\rangle \tag{3}$$

and a simultaneous second-order energy correction

$$E_K^{(2)} = \langle\Psi_K^{(0)}|H'|\Psi_K^{(1)}\rangle \tag{4}$$

where Φ_a is a perturber CSF belonging to the First Order Interaction Space (FOIS), as determined by all the CSFs included in the variational space $\{V\}$. The energies in the denominator are eigenvalues of some unperturbed Hamiltonian H_0, whereas the operator H' is the perturbation Hamiltonian. Hence, the complete Hamiltonian is $H = H_0 + H'$.

Both Møller−Plesset (MP) and Epstein-Nesbet (EN) partition schemes are implemented, although the former gives in general better results and has the advantage that the zero-order Hamiltonian is a one-body operator. The MP unperturbed operator corresponds to the diagonal part of the Fock operator which in second quantization formalism may be written as

$$H_0^{\mathrm{MP}} = \sum_r F_{rr} a_r^\dagger a_r \tag{5}$$

where the a's are the usual creator/annihilation operators, and F is the Fock matrix arising from the HF wave function. This leads to the so-called barycentric approximation[21] where the zero-order states are eigenfunctions of H_0^{MP} and the unperturbed energy is

$$\varepsilon_K = \langle\Psi_K^{(0)}|H_0^{\mathrm{MP}}|\Psi_K^{(0)}\rangle = \sum_i^{\{V\}} |C_{iK}|^2\langle\Phi_i|H_0^{\mathrm{MP}}|\Phi_i\rangle = \sum_i^{\{V\}} |C_{iK}|^2\varepsilon_i \tag{6}$$

The barycentric approximation simplifies the problem, avoiding the solution of large-scale linear equation systems.[31,32] In the Epstein-Nesbet partition, the unperturbed Hamiltonian is conveniently defined through a diagonal projected Hamiltonian

$$H_0^{\mathrm{EN}} = \sum_K^{\{V\}} |\Psi_K^{(0)}\rangle\langle\Psi_K^{(0)}|H|\Psi_K^{(0)}\rangle\langle\Psi_K^{(0)}| + \sum_p^{\{\mathrm{FOIS}\}} |\Phi_p\rangle\langle\Phi_p|H|\Phi_p\rangle\langle\Phi_p| \tag{7}$$

so that both the CI states and the CSFs belonging to the FOIS are eigenvectors of H_0^{EN}. Although in the above equation the sum over K is formally on all the eigenvalues of the projected Hamiltonian, in practical cases the sum can be restricted to the computed zero-order states. With this choice, the MP and EN partition schemes only differ for the denominators, whose calculation is obviously heavier in the EN case.

The perturbative FOIS space derives from the orbitals in the current active space, so that inactive orbitals are completely ignored in the perturbative calculation. This step allows for a selection of a given number of ONCs, which might be included in the variational space employed in a subsequent CI step. The selection can be performed by using different criteria, possibly depending on the property under investigation.[33] The criteria can be second-order energy contribution, contribution to the

DOI: 10.1021/ct501071k
J. Chem. Theory Comput. XXXX, XXX, XXX−XXX

first-order wave function, energy difference between a pair of states, and contribution to a given one-electron property.

Despite the efficient parallelization, the perturbative step may be time-consuming and the calculation can become quickly unfeasible even for molecules of moderate size when large active spaces are considered. The standard way to overcome this difficulty is to adopt an internal contraction scheme[34,35] that drastically reduces the number of perturbers. Unfortunately, this scheme is only suitable for CAS wave functions and also creates additional complications due to the nonorthogonality of the perturbative states. For this reason BALOO adopts a different strategy, allowing the user to impose some restrictions on the FOIS, depending on the property of interest. For instance, for the calculation of excitation energies of closed shell molecules, the perturbers with excitation level above 7 do not appreciably affect the results. Likewise the number of unpaired electrons in the perturbers may be limited to 8 or 10 without affecting the energy differences. These restrictions imply a very large saving in term of computational cost.

A further strategy to save CPU time is the selection of a subspace in the variational space, which is able to represent on equal footing all the states considered, to be used as the generator space for the FOIS. This method was already implemented in the CIPSI perturbative algorithm[23] and represents a very useful strategy mainly for large variational spaces, where the number of very small coefficients of the CI states is rather high. In practice the FOIS coincides with the perturbative space and is determined by the following formula

$$\{\mathrm{FOIS}\} = (\hat{S} + \hat{D})\{V'\} \tag{8}$$

where $\hat{S}$ and $\hat{D}$ are the single and double substitution operators, and $\{V'\}$ is the smallest subspace of the full variational space $\{V\}$ for which the norm of the projection of all the CI states in this space is higher than a given value τ. If N_S is the number of CI states, then

$$\sum_{i}^{\{V'\}} \left|C_{iK}^{(0)}\right|^2 > \tau \quad \forall\ K = 1...N_S \tag{9}$$

where the C's are the expansion coefficients of the CI states given in eq 2. In other words if P' is the projector into $\{V'\}$, such subspace includes the minimum number of elements of $\{V'\}$ for which the following equation is verified for all CI states

$$\langle P'\Psi_K^{(0)}|P'\Psi_K^{(0)}\rangle > \tau \tag{10}$$

The same strategy can be used for the calculation of the Hamiltonian matrix elements between the unperturbed CI states and the perturbers, that is the basic quantity for the perturbative calculation. The subspace $\{V'\}$ is chosen in eq 9 so that the equation

$$\langle P'\Psi_K^{(0)}|H'|\Phi_a\rangle \cong \langle \Psi_K^{(0)}|H'|\Phi_a\rangle \tag{11}$$

is approximatively satisfied. It has been verified that in practical cases the value of τ indicates the accuracy of the perturbative energies, namely $\tau = 1-10^{-n}$ implies an accuracy of about n significant digits. Therefore, the reasonable choice of $n = 5$ does not affect appreciably the quality of the energy result while decreasing the CPU time by 10 or 20 times, depending on the calculation and on the number of CI states. Both these projections are controlled by suitable variables that can easily be defined in BALOO's input.

CSPA Step. The restriction of the active space can be removed in the CSPA step, which performs a perturbative calculation including excitations involving also the inactive orbitals. This is generally the last step of the calculation sequence and, depending on the dimension of the active and inactive spaces, may be rather time-consuming. Similarly to previous steps, it has been parallelized to scale almost linearly with the number of processors. The only restriction to the number of CPUs is in the memory demand, as each thread needs to store the requested two-electron integrals.

Diagrammatic Perturbative Step. A valid alternative to CSPA is offered by the diagrammatic perturbative step described in the following. According to the pioneering paper of Cimiraglia,[28] the perturbative calculation can be performed using diagrammatic techniques, with large performance improvements. In the present version the improvement with respect to traditional perturbation is essentially due to a simpler way to incorporate two-electron integrals in the perturbative energy calculation, i.e. without the explicit use of CSFs or SDs. Differently from the original implementation, which considers separately the perturbative energy diagrams, in the present code all diagrams are automatically evaluated in symbolic form and collected in a number of terms. Similarly to the technique used for the Hamiltonian matrix elements, the diagrammatic terms are stored in memory once for all and retrieved when needed. Likewise the other steps and differently from the original proposal,[28] the diagrammatic step works both for CSFs and SDs. Moreover the same strategies described in the perturbative step and aimed to save CPU time without affecting the quality of the results can be adopted also in this step.

The current diagrammatic code is able to dramatically decrease the CPU time. As an example, on 24 CPU processors Intel E5-2620 the calculation for guanine with the 6-311G(d)+ basis set leading to 246 MOs (excluding core MOs) with a CI space of 45,000 CSF and 2×10^{11} perturbers takes 210 h for the traditional perturbation complemented with CSPA and only 5.2 h for the diagrammatic perturbation, i.e. a reduction of about 40 times. On the other hand, the diagrammatic perturbation can only be used for energy calculation, and, as CSFs are never explicitly considered, it cannot conveniently be used for the selection of ONCs, necessary to efficiently enlarge the variational space. A further improvement (not considered in the above timings) comes from the extrapolation procedure already implemented in CIPSI[36] which allows for further CPU time reduction, without appreciably affecting the accuracy of the results.

Finally it should be noticed that the current diagrammatic implementation in BALOO works for the FOIS projected on the active orbitals as well as for the FOIS coming from the whole set of orbitals (active+inactive). Thus, the diagrammatic perturbative step can be equivalent to traditional perturbation plus the CSPA step.

Both in diagrammatic, CSPA and standard perturbative steps the Quasi Degenerate Perturbation Theory (QDPT) based on an effective Hamiltonian is implemented in the barycentric MP partition. The model space is formed by the states selected in the CI step, and the fluctuation potential perturbation is computed up the second order. Whereas in many cases QDPT does not improve appreciably the results, there are situations in which the nondiagonal perturbative couplings are strong and the results are rather different from those arising from nondegenerate perturbation theory. A typical example is

DOI: 10.1021/ct501071k
J. Chem. Theory Comput. XXXX, XXX, XXX−XXX

Table 1. Vertical Excitation (Vex) Energies (eV) of Azomethane by BALOO and Compared with Those of Ref 58[a]

	EOMEE-CCSD[58]		CC3[58]			BALOO		
assign	vex	osc. str.	vex	osc. str.	exp[59,60]	vex	osc. str.	assign
$n_+ \rightarrow \pi^*$	3.77	0	3.76	0	3.6	**3.41**	0	$n_+ \rightarrow \pi^*$
$n_+ \rightarrow R_{3s}$	6.27	0	6.20	0	5.5	5.88	0	$n_+ \rightarrow R$
$n_+ \rightarrow R_{3p}$	**6.74**	**0.08**	**6.65**	**0.08**		**6.46**	**0.08**	**n+ → R**
$n_+ \rightarrow R_{3p}$	**6.94**	**0.14**	**6.90**	**0.15**	**6.8**	**6.67**	**0.14**	**$n_+ \rightarrow R$**
$n_+ \rightarrow R_{3p}$	6.97	0.04	6.92	0.05		6.68	0.04	
$n_+ \rightarrow R_{3d}$	7.49	0	7.42	0		6.99	0.01	$n_- \rightarrow \pi^*$
$n_+ \rightarrow R_{3d}$	7.64	0	7.58	0		7.12	0	$n_+ \rightarrow R$
$n_+ \rightarrow R_{3d}$	7.76	0	7.71	0		7.26	0	$n_+ \rightarrow R$
$n_- \rightarrow \delta^*$	7.60	0.01	7.30	0.01		7.38	0	$n_+ \rightarrow \pi^*$
$n_+ \rightarrow R_{3d}$	8.39	0	8.33	0		8.06		
$n_+ \rightarrow R_{4p}$	8.40	0.05	8.38	0.13				
$n_+ \rightarrow 2\pi^*$	8.68	0	8.62	0				
$\pi \rightarrow \pi^*$	**8.60**	**0.25**	**8.27**	**0.20**	**8.0**	**8.09**	**0.32**	**$\pi \rightarrow \pi^*$**
$n_+ \rightarrow R_{4p}$	8.97	<0.01	8.91	?		8.83	0.01	$n_+ \rightarrow R$
$\pi \rightarrow R_{3s}$	9.05	0.05	8.97	?	8.7	8.92	0	$\pi \rightarrow R$
$\sigma \rightarrow \pi^*$	9.10	0	8.92	0		9.31	0	$\pi \rightarrow R$

[a]The most intense excitations are reported in boldface.

provided in ref 37 for the energy crossing between the neutral and ionic configurations in NaCl.

Property Computation. BALOO can compute a number of one-electron properties as well as a full excitation spectrum if many states of the same spin are requested in the calculation. This requires the evaluation of the one-body density matrices for both single-state and two-state transitions, which can be currently performed at two levels of approximation: zero-order density matrices using the CI states and first-order perturbed density matrices.[38] Natural orbitals of a specific state or of a state-average can be next computed and written on disk to be possibly retrieved by the IJKL program for integral transformation, in order to repeat CI+PT calculation with an (hopefully) improved set of MOs.

Protocol for Magnetic Interactions in Diradicals. The BALOO software allows for CI calculations to be performed within the Difference Dedicate Configuration Interaction (DDCI) scheme,[39,40] originally implemented by some of us in the original CIPSI code.[41−49] Furthermore, in order to reliably investigate spin coupling in diradicals, an accurate yet feasible computational protocol within the DDCI scheme has been proposed in the past few years by our group,[45,46] and it is now implemented in BALOO. All details can be found in the quoted references, whereas only a brief summary will be given in the following. (i) A starting set of MOs is obtained at the SCF level for the target molecule in its triplet state by a ROHF calculation using a modified version of GAMESS;[50] (ii) the canonical SCF MOs are localized[44] onto specific molecular moieties, and only the most relevant to the magnetic interaction are retained in the variational calculation; (iii) a suitable one-electron operator is built in this space and diagonalized, in order to obtain new modified MOs able to improve the convergence of the DDCI calculation vs the number of virtual MOs;[44] (iv) the CSPA,[48] based on a balanced combination of variational and perturbative calculations within the DDCI selection, is finally employed to yield accurate values for the singlet−triplet energy gap or for the J term of the Heisenberg−Dirac−Van Vleck model. This protocol has been successfully applied to diradical species, usually made by two "magnetic" fragments, each bearing one unpaired electron, bridged by an unsaturated organic moiety, polyene or aromatic. For such target molecules, the DDCI is built in terms of the minimal CAS(2,2) space associated with the two magnetic orbitals (one on each "magnetic" fragment) plus all the determinants arising from single and double excitations from the magnetic to the virtual orbitals, and all the double excitations from the core orbitals involving only one core-to-virtual excitation (see also Figure 3 of ref 51 or Table 1 of ref 46). This type of calculation is usually performed using SD as this allows to include both singlet and triplet states in a unique calculation. However, CSF could be used without increasing appreciably the total wall time.

Protocol for Excited States. The calculation of excited states and absorption spectra can be performed according to the route that in the past has been used with success[52−55] with the CIPSI method.[56] After obtaining a suitable MOs set, by an HF calculation using a modified version of GAMESS and after the integral transformation with IJKL is accomplished, we start the BALOO calculation with a modest variational space of singly excited ONC which is gradually enlarged by three of four CI+PT steps, until the calculation reaches large but still feasible dimensions. The final fourth step includes a diagrammatic perturbative calculation followed by the calculation of the oscillator strengths. The selection of the ONCs to be used to enlarge the variational space is usually based on energy criteria.

Spectral Line-Shapes. Due to the efficiency and speed of BALOO, we can afford with a reasonable computational cost the calculation of the line shape profile of the electronic absorption bands, exploiting the results of molecular dynamics. This can be performed by following a sequential approach, essentially consisting in applying the protocol for the excited state calculation described above to a set of snapshots randomly selected from a purposely stored trajectory, in which the time evolution of the system is described by a force field. The final spectrum is then obtained by a simple average of the stick spectra (frequency and oscillator strength) obtained for every single snapshot. If each stick spectrum is separately convoluted with a Gaussian function, the above-mentioned average also yields a spectral line shape that can be directly compared with the experiment.

DOI: 10.1021/ct501071k
J. Chem. Theory Comput. XXXX, XXX, XXX−XXX

RESULTS AND DISCUSSION

All geometry optimizations were performed using the GAUSSIAN09[57] package by means of density functional theory (DFT). The employed combination of functional/basis set will be given in the following for each investigated case study.

Absorption Spectra. In this section the BALOO performances in the calculation of excited states and electronic absorption spectra will be discussed. We have considered two different test cases, namely azomethane and pyrimidine.

Azomethane. The program is first tested on azomethane *in vacuo*, because this system has been recently studied[58] by very accurate post-HF methods, thus representing a good benchmark for validating our results. Moreover experimental results are also available.[59,60]

The first 15 excitation energies and oscillator strengths obtained for the planar optimized molecular geometry of ref 58 using the aug-cc-PVDZ basis set are reported in Table 1. The resulting absorption spectrum is shown in Figure 1. In the MRCI calculation we have taken all orbitals, except the 1s of carbon and nitrogen. After five CI+PT2 steps the final CI space includes 250,280 CSFs. The time needed for such calculation on a 32 processor (Xeon E5-2670 2.60 Ghz) workstation was roughly 2.5 days.

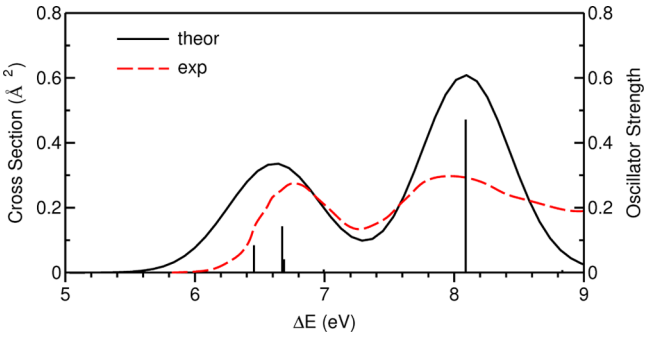

Figure 1. Computed (sticks and continuous line, black) and experimental[59,60] (dashed line, red) spectra of azomethane. The line shape profile is obtained by a convolution with a Gaussian function of fwhm = 0.80 eV.

In Figure 1 we can see a good agreement between experimental and theoretical predictions, which is confirmed by the values reported in Table 1.

The difference in the vertical excitation energies of the most intense peaks is smaller than 0.2 eV. The maximum error is found for the band at 5.5 eV whose precise detection presents some experimental problems due to its very small intensity. The comparison between the present results and those of ref 58 is globally good, although some differences are observed especially for the intense band centered at 8 eV which we found to be concentrated in a single electronic state, whereas EOM-CCD and CC3 calculations predict a splitting in two bands. Moreover our excitation energy seems to be more accurate.

Pyrimidine. The computational feasibility of the BALOO protocol for excited states has been further tested by averaging the stick spectra computed for a large number of geometries issuing from molecular dynamics (MD) simulations. As a test case, we have exploited a recent MD simulation,[61] performed for the pyrimidine molecule in gas phase at 298 K, using a force-field (FF) purposely parametrized for pyrimidine[61] through the JOYCE[62,63] procedure.

One hundred frames (one every 50 ps) were extracted from the MD trajectory, and each of them was used for a single CI-MRPT2 calculation. Finally, all the computed transition frequencies and oscillator strengths are convoluted with Gaussian functions and subsequently averaged into a unique band. The resulting broadening hence accounts, at a classical level, for the nuclear dynamics.

These calculations have been performed using the 6-311G(d) basis set so that, neglecting the 1s orbitals of carbon and nitrogen atoms, the MOs transformed from atomic to molecular basis and included in the construction of the CI space are 120, 15 doubly occupied and 105 empty. Each calculation of 25 eigenstates, which cover the VUV region up to 10 eV, with a final CI space of about 50,000 CSF, requires roughly 6 h on a 16 processors (Xeon 2.60 GHz) workstation, including the final perturbative diagrammatic second-order energy correction to the CI eigenvalues.

The computed spectrum is reported in Figure 2 and compared with the recent high resolution measurements in the gas phase of ref 64. In agreement with the conclusions of refs 61 and 65, four bands appear at energies below the most intense $\pi \rightarrow \pi^*$ transition (at ~8 eV), which can be assigned as reported in Table 2. Above the $\pi \rightarrow \pi^*$ band the last absorption below 10 eV is characterized by a series of $n \rightarrow \pi^*$ transitions with small oscillator strengths.

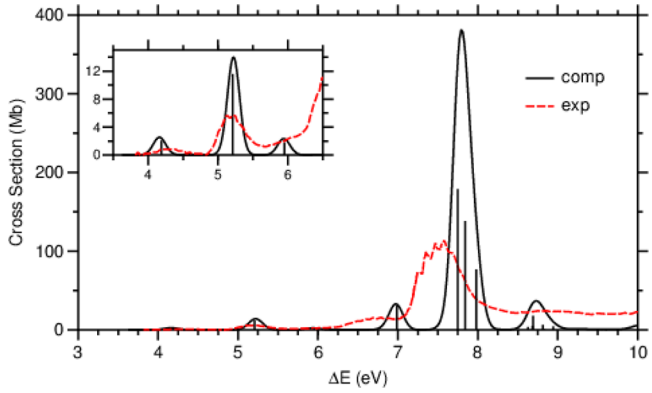

Figure 2. Computed and experimental[64] spectra of pyrimidine. The line shape profile is obtained by a convolution of each line of the 100 spectra with a Gaussian function of fwhm = 0.2 eV.

Table 2. Bands Head Energies (eV) of Pyrimidine as Obtained by the Average of BALOO Computations on 100 MD Snapshots

assign	exp.[60]	BALOO
$n \rightarrow \pi^*$	4.2	4.1
$\pi \rightarrow \pi^*$	5.2	5.2
$n \rightarrow \pi^*$	5.9	5.9
$\pi \rightarrow \pi^*$	6.7	6.9
$\pi \rightarrow \pi^*$	7.5	7.8

The comparison between experimental and computational results displayed in Figure 2 shows a good agreement in the position of the bands, including the shoulder at 5.9 eV (see inset), although for the strongest $\pi \rightarrow \pi^*$ band (that observed at 7.5 eV) the shift is larger (0.3 eV). The discrepancy found for the band at 7.5 eV, as well as those found in width and intensity of the bands, are probably due, as discussed in refs 61 and 65,

DOI: 10.1021/ct501071k
J. Chem. Theory Comput. XXXX, XXX, XXX−XXX

to the lack of quantum vibronic effects, which are smeared out at least partially in solution, where molecular dynamics appears to be able to simulate the effects on the bandwidth of solute−solvent interactions.[65]

Test on Intensive Properties (Weak Separability). It is well-known that despite the Rayleigh−Schrödinger perturbative method being able to give extensive energies, for multireference wave functions as unperturbed states, the size consistency of the perturbative energies is generally not obtained. Moreover, if the system is composed of two noninteracting subsystems, multiplicative separability of the wave function is not guaranteed, although no *a priori* truncation is imposed on the variational space. Even in the case the variational wave functions satisfy the multiplicative separability, small deviations from additive energies may be observed. Such defects propagate also on the intensive properties of the monomers as the excitation energies (weak separability). However, we may reasonably expect that the deviations from intensive and extensive scaling properties are less and less relevant with the increasing of the variational space. This is because the projected CI wave functions resemble more and more the full CI ones, and the subsequent perturbative treatment should further improve the scaling properties.

To verify the error on the weak separability requirement, we have performed a number of calculations on a noninteracting dimer composed of NH_3 and CH_3OH. The excitation energies of the former with and without the methanol molecule have been computed according to the standard protocol of BALOO for the calculation of excitation spectra, carried out with the 6-31G* basis set. In the post HF calculations, all the 1s orbitals have been frozen. In both calculations, using the CIS space as the starting CI space, the variational space is gradually enlarged in three steps by a given factor referred to the number of ONCs. The final number of CSF is 239,790 for NH_3 and 212,011 for the dimer. For ammonia, the CI-MRPT2 calculation of the excitation energies gives practically the full CI result, as they do not change from the two last steps and the MP and EN excitation energies are identical. Therefore, these values can be used as a reference for the calculations on the dimer. The results are displayed in Table 3.

Table 3. Comparison of the Excitation Energies of Ammonia with and without a Noninteracting Methanol Molecule, as Computed by the BALOO Program[a]

parameter	value		
ammonia spectrum (isolated system)	8.18	10.53	14.10
ammonia-methanol 17,300	8.33	10.70	14.25
ammonia-methanol 51,486	8.32	10.68	14.23
ammonia-methanol 83,476	8.27	10.63	14.18
ammonia-methanol 130,026	8.26	10.60	14.17
ammonia-methanol 212,011	8.23	10.58	14.15

[a]The excitation energies (eV) of the isolated ammonia are displayed in the first row. The remaining rows report the excitation energies of ammonia in the dimer at CI+Pert level, for gradually enlarged variational spaces. The number in the first column is the number of CSF in the variational space, which provides the zero-order states for the subsequent perturbative calculation.

It is apparent that as the variational space increases, the excitation energies of the ammonia in the dimer approach monotonically to the exact values. However, the convergence is not so quick, and in the best calculation the MR perturbative results agree with the reference values within 0.05 eV. The data reported confirm that the intensive properties can be computed with acceptable accuracy only in the case of large variational spaces, for which deviations of the wave function from the multiplicative separability requirement is small enough.

Molecular Magnets. One of the major strengths of the BALOO code stands in the possibility of accurately computing critical observables (e.g., magnetic couplings) with an affordable computational cost. This can be done thanks to the implementation of specific protocols, namely DDCI and CSPA. Two different tests have been devised to illustrate the accuracy and feasibility of BALOO computations. First, the accuracy in predicting singlet−triplet energy gaps, will be tested on different homologues of benzyne diradicals, a popular benchmark[66−69] for this kind of calculations. Next, the possibility of performing calculations on large molecules containing metal centers will be validated on transition metal-based molecular magnets.

Benzynes. All three isomeric benzyne diradicals, i.e. *o*-, *m*-, and *p*-benzyne (see Figure 3), have been the object of several studies in the last years, by both theoretical[66−82] and experimental[83−88] points of view due to important applications in synthesis, and the remarkable role in the action of antitumoral compounds, together with the computational challenges connected to their peculiar structure. Among others, the singlet−triplet splitting ΔE_{TS} of such compounds have become a reference value for benchmarking high-level multireference methods.[66−68] Furthermore, reliable experimental

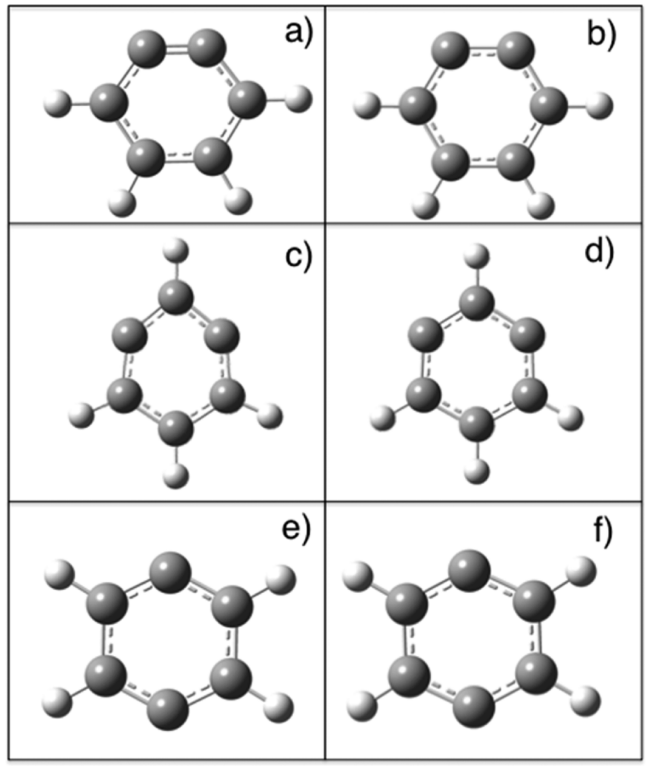

Figure 3. Geometries were taken from ref 67, where the internal coordinates for *o*- and *m*-benzyne were obtained through RHF-CCSD(T) and UHF-CCSD(T) optimizations for singlet (a and c panels) and triplet states (b and d panels), respectively, whereas the singlet (e panel) and triplet (f panel) states of *p*-benzyne were optimized using broken symmetry orbitals and cc-pVDZ/UHF-CCSD(T) wave functions.

DOI: 10.1021/ct501071k
J. Chem. Theory Comput. XXXX, XXX, XXX−XXX

Table 4. Computational Routes Employed for the Calculations of the Magnetic Splitting ΔE_{TS} in Benzyne Homologues

SCF Calculations		
singlet		triplet
orbitals computed at the ROHF/6-311G* level for the triplet, at the singlet geometry, G_S		orbitals computed at the ROHF/6-311G* level, at the triplet geometry, G_T
BALOO Calculations		
DDCI/V	DDCI/A	DDCI+PT2/A
$\Delta E_{TS} = [E-E_S]@G_S$	$\Delta E_{TS} = [E_T]@G_T - [E_S]@G_S$	$\Delta E_{TS} = [E_T + dE_T^{PT2}]@G_T - [E_S+dE_S^{PT2}]@G_S$

estimates[85] of ΔE_{TS} have been reported and can also be employed in testing the accuracy of the results.

A detailed discussion on *m*-benzyne singlet and triplet state's equilibrium geometries has been recently reported in refs 81 and 82. However, for a reliable comparison with the reference theoretical data reported in ref 67 for all the benzyne homologues, molecular geometries were taken from there, where all the details concerning the optimization procedure and the numerical values of the optimized coordinates can be found. The employed molecular geometries for all the considered systems are displayed in Figure 3 for both spin states. Even from a preliminary visual inspection, it appears that the investigated diradicals, especially *o*- and *m*-isomers, have rather different equilibrium geometry in the singlet (G_S) and triplet (G_T) states.

Three different computational routes were devised to estimate the effect of such geometry distortions on ΔE_{TS} (see Table 4). The first route (DDCI/V) corresponds to the standard "vertical" approach, successfully employed for many organic diradicals,[41−49] where the geometry distortions are ignored and a DDCI calculation for both the triplet and singlet states is here carried out at the equilibrium geometry G_S of the singlet (taken from ref 67), which is the ground state of all three isomers. On the contrary, the second protocol (DDCI/A) corresponds to the adiabatic approximation as it takes into account the geometry distortion: the singlet and triplet energies are computed at the DDCI level separately for G_S and G_T, respectively, and ΔE_{TS} is computed as the difference of the two resulting values. Following route (DDCI+PT2/A) we can further refine the DDCI/A result, by adding a perturbative step to the DDCI states as obtained in step DDCI/A, thus increasing the accuracy of the computed energies.

The resulting energy gaps, obtained through the different computational routes, are reported in Table 5, together with the most accurate values available in the literature.[66−68] As far as the most accurate route DDCI+PT2/A is concerned, it appears that the magnetic gaps are well reproduced for all three homologues, the computed value being in excellent agreement with both experimental measures[85] and high-level computational results.[66−68] Incidentally, it is noteworthy that the computed ΔE_{TS} for *p*-benzyne of 5.3 kcal/mol confirms the sqic-MRCCSD estimate (5.2 kcal/mol), hence giving further support to the hypothesis of an alternative experimental assignment of 5.5 kcal/mol.[67] For the DDCI/A results only slightly different values were obtained for all three isomers with respect to the experimental values, being in some cases (e.g., *m*-benzyne) even in quantitative agreement.

Table 5. Singlet Triplet Energy Gaps ΔE_{TS} for Benzyne Homologues[a]

method	ref	*p*-benzyne	*m*-benzyne	*o*-benzyne
Literature				
REKS/6-31G(d)	66	4.1	21.6	36.5
MkCCSD	67	4.5	18.7	35.1
sqic-MRCCSD/cbs+zpe	68	5.2		
BALOO				
DDCI/V	this work	5.1	33.4	50.6
DDCI/A	this work	4.8	21.1	39.2
DDCI+PT2/A	this work	5.3	19.7	36.9
Experimental				
exp	85	3.8 (5.5?)	21.0	37.5

[a]All values are in kcal/mol.

By looking at the average computational times needed for each computational route, reported in Table 6, it is evident that the DDCI/A route should be followed, at least for *m*- and *o*-benzynes. On the contrary, since the difference between G_S and G_T *p*-benzyne geometries is very small, route DDCI/V already gives a very reasonable estimate of ΔE_{TS}. Hence, when dealing with larger homologues, computational convenience suggests that the standard route DDCI/V could be used for *p*-benzyne, although also the DDCI/A route could remain feasible.

Table 6. Computer Times Employed for the ΔE_{TS} Calculations According to the Different Routes

route	time
DDCI/V	2 h
DDCI/A	4 h
DDCI+PT2/A	5 days

Metallic Biradical. As an example of metallic diradical, we have considered the bis(*μ*-azido)tetrakis(4-*tert*-butylpyridine)-dicopper(II) dication, prepared and studied in 1983 by Khan and co-workers[85,89] (Figure 4). The species was found ferromagnetic (triplet ground state) with a value of $J = 105 \pm 20$ cm^{-1}.

All the calculations have been performed using the 10-electron ECP of Hay and Wadt[90−92] for copper with its DZ basis and the 6-311G basis set for the remaining atoms. The geometry has been fully optimized for the lowest triplet state at the DFT/B3LYP level. For purposes of comparison, some key bond distances and angles are reported in Table 7.

The two MOs bearing an unpaired electron are the symmetric and antisymmetric combination of Cu in plane d orbitals with a little contribution of p orbitals of the bridging N and of the pyridine N. Fragmentation-localization is used to only retain the MOs on the $Cu(N_3)_2Cu$ part of the whole cation (delimited by red lines in Figure 4).

The resulting orbital space used for the DDCI-CSPA calculation is then made by 32 double occupied, 2 singly occupied (magnetic), and 65 empty MOs. Taking all the occupied and 50 of the 65 empty orbitals for the variational part of the calculation (dimension of the CI matrix of 775,209 Slater determinants), we obtain a triplet ground state and a value of $E_S - E_T = 130.1$ cm^{-1}. The full variational calculation (all 65 empty MOs and dimension of the CI matrix of 1,228,681) gives

DOI: 10.1021/ct501071k
J. Chem. Theory Comput. XXXX, XXX, XXX−XXX

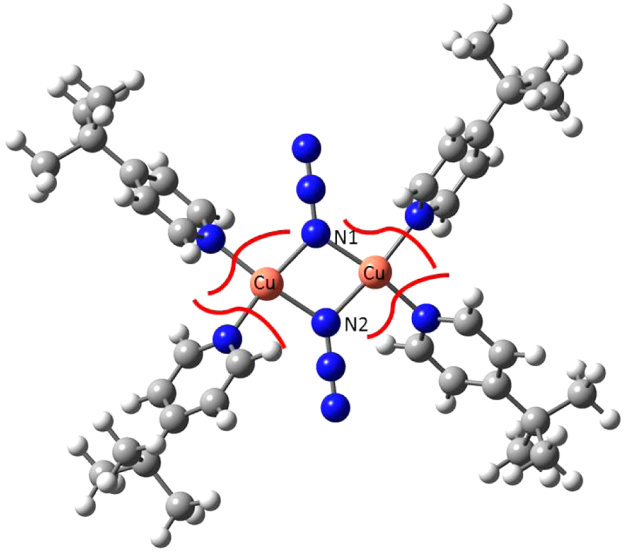

Figure 4. Cu-based dication diradical. The red lines indicate the fragmentation made in the calculation.

Table 7. Selected Distance and Angles for Bis(μ-azido)tetrakis(4-*tert*-butylpyridine)dicopper(II) Dication[a]

distances (Å) and angles (deg)	optimized	exptl[82,83]
R_{Cu-Cu}	3.13	3.04
$R_{Cu-N1} = R_{Cu-N2}$	2.01	1.99
R_{N1-N2}	2.52	2.53
N1−Cu−N2	77.6	79.5
Cu−N1−Cu = Cu−N2−Cu	102.4	100.5
$E_S - E_T$ (cm^{-1})	130.1	105 ± 20

[a]In the last row the comparison of the experimental and computed value of the singlet−triplet energy gap is also reported. The ground state is the triplet state.

exactly the same value, in very good agreement with the experimental data of 105 ± 20 cm^{-1}.

CONCLUSIONS

The present study is the first systematic assessment of BALOO performances for different problems involving significant static and dynamic correlation at the same time. In our opinion, the presented test cases show that, thanks to a number of conceptual and technical developments, BALOO is a fast, robust, and versatile code for accurate multireference computations. This result has been obtained through full parallelization of the code, optimization of the integral transformation, implementation of the diagrammatic version of perturbation theory, flexible manipulation (localization, fragmentation, etc.) of orbitals, effective computation of properties using the density matrix perturbed to the first order, and extension of the DDCI concept to different properties including more effective orbital selection.

Despite these strong features, some weak points remain, which call for further analysis. First of all, we recall that, even in the case the reference wave functions satisfy the multiplicative separability requirement, the correlation energy provided by the present perturbation step is not size consistent. Several test studies have shown that this issue is usually not too serious and can be taken under control by empirical recipes like the generalized Davidson correction.[93] However, a more general solution of this problem would be welcome, for instance replacing the linear CI model by a nonlinear (nearly) size-consistent modification. The second weakness of the model is that it is not completely a "black-box" procedure because it requires the choice of a suitable reference space. Although this choice is, in a sense, automatically improved by the iterative extension of the reference space, it remains true that some intervention by the user is required. We consider this aspect a strength of the method since the choice can be based on chemical intuition and/or previous experience, thus being intrinsically connected with the (sought for) large flexibility of the approach. Third, the method does not lead in principle to microscopically smooth potential energy surfaces due to the truncation procedures employed. However, continuity can be enforced by means of techniques based, for instance, on overlap between the wave functions of neighboring points. Additional work must be performed, in our opinion, in this direction. Fourth, the selection of active orbitals and target excited states has sometimes troubles for large basis sets including diffuse functions. Also here further analysis is needed, but some preliminary results show that approaches based on population analysis, shape of the orbitals, and energy shifts can be profitably used.

In any case the overall performance of Baloo for the calculation of excitation energies and magnetic properties is already satisfactory, and this is encouraging for the further developments of the method that are presently under investigation.

As a final remark, we should point out that other methods, such as those based on the density matrix renormalization group (DMRG),[94−96] are currently under development, with the aim of investigating large molecular systems by multi-reference calculations.

ASSOCIATED CONTENT

Supporting Information

Additional data and several details about the reported calculations not included in this paper. This material is available free of charge via the Internet at http://pubs.acs.org.

AUTHOR INFORMATION

Corresponding Author

*E-mail: ivo.cacelli@unipi.it.

Notes

The authors declare no competing financial interest.

ACKNOWLEDGMENTS

The research leading to these results has received funding from the European Union's Seventh Framework Programme (FP7/2007-2013) under grant agreement no. ERC-2012-AdG-320951-DREAMS. This work was also supported by Italian MIUR (PRIN 2010-2011, 2010FM738P, and 2010PFLRJR)

REFERENCES

(1) Raghavachari, K.; Trucks, G. W.; Pople, J. A. A fifth-order perturbation comparison of electron correlation theories. *Chem. Phys. Lett.* **1989**, *157*, 479−483.

(2) Heckert, M.; Kállay, M.; Tew, D. P.; Klopper, W.; Gauss, J. Basis-set extrapolation techniques for the accurate calculation of molecular equilibrium geometries using coupled-cluster theory. *J. Chem. Phys.* **2006**, *125*, 044108.

(3) Stanton, J. F.; Bartlett, R. J. The equation of motion coupled-cluster method. A systematic biorthogonal approach to molecular

DOI: 10.1021/ct501071k
J. Chem. Theory Comput. XXXX, XXX, XXX−XXX

excitation energies, transition probabilities, and excited state properties. *J. Chem. Phys.* **1993**, *98*, 7029−7039.
(4) Marques, M. A. L.; Ullrich, C. A.; Nogueira, F.; Rubio, A.; Burke, K.; Gross, E. K. U. *Time-Dependent Density Functional Theory*; Springer-Verlag: 2006; Vol. *706*, p 555.
(5) Murphy, R. B.; Messmer, R. P. Generalized Møller-Plesset perturbation theory applied to general MCSCF reference wave functions. *Chem. Phys. Lett.* **1991**, *183*, 443−448.
(6) Roos, B. O. Theoretical Studies of Electronically Excited States of Molecular Systems Using Multiconfigurational Perturbation Theory. *Acc. Chem. Res.* **1999**, *32*, 137−144.
(7) Pierloot, K. Transition metals compounds: Outstanding challenges for multiconfigurational methods. *Int. J. Quantum Chem.* **2011**, *111*, 3291−3301.
(8) Szalay, P. G.; Müller, T.; Gidofalvi, G.; Lischka, H.; Shepard, R. Multiconfiguration Self-Consistent Field and Multireference Configuration Interaction Methods and Applications. *Chem. Rev.* **2012**, *112*, 108−181.
(9) Roos, B. O.; Malmqvist, P.-Å. Relativistic quantum chemistry: the multiconfigurational approach. *Phys. Chem. Chem. Phys.* **2004**, *6*, 2919−2927.
(10) Nakano, H.; Nakatani, J.; Hirao, K. Second-order quasi-degenerate perturbation theory with quasi-complete active space self-consistent field reference functions. *J. Chem. Phys.* **2001**, *114*, 1133−1141.
(11) Davidson, E. R.; Jarzecki, A. A. Recent Advances in Multireference Methods. In *Recent Advances in Computational Chemistry*; Hirao, K., Ed.; World Scientific: Singapore, 1999; Vol. *4*, p 31.
(12) Buenker, R. J.; Peyerimhoff, S. Individualized configuration selection in CI calculations with subsequent energy extrapolation. *Theor. Chim. Acta* **1974**, *35*, 33−58.
(13) Buenker, R. J.; Peyerimhoff, S. Energy extrapolation in CI calculations. *Theor. Chim. Acta* **1975**, *39*, 217−228.
(14) Rolik, Z.; Szegedy, L.; Ladjánszki, I.; Ladóczki, B.; Kállay, M. An efficient linear-scaling CCSD(T) method based on local natural orbitals. *J. Chem. Phys.* **2013**, *139*, 094105.
(15) Andersson, K.; Malmqvist, P. Å.; Roos, B. O.; Sadlej, A. J.; Wolinski, K. Second-order perturbation theory with a CASSCF reference function. *J. Phys. Chem.* **1990**, *94*, 5483−5488.
(16) Andersson, K.; Malmqvist, P. Å.; Roos, B. O. Second-order perturbation theory with a complete active space self-consistent field reference function. *J. Chem. Phys.* **1992**, *96*, 1218−1226.
(17) Angeli, C.; Cimiraglia, R.; Evangelisti, S.; Leininger, T.; Malrieu, J. P. Introduction of n-electron valence states for multireference perturbation theory. *J. Chem. Phys.* **2001**, *114*, 10252−10264.
(18) Angeli, C.; Pastore, M.; Cimiraglia, R. New perspectives in multireference perturbation theory: the n-electron valence state approach. *Theor. Chem. Acc.* **2007**, *117*, 743−754.
(19) Neese, F. A spectroscopy oriented configuration interaction procedure. *J. Chem. Phys.* **2003**, *119*, 9428−9443.
(20) Schapiro, I.; Neese, F. SORCI for photochemical and thermal reaction paths: A benchmark study. *Comput. Theor. Chem.* **2014**, *1040*, 84−98.
(21) Huron, B.; Malrieu, J.-P.; Rancurel, P. Iterative perturbation calculations of ground and excited state energies from multiconfigurational zero-th order wavefunctions. *J. Chem. Phys.* **1973**, *58*, 5745−5759.
(22) Evangelisti, S.; Daudey, J. P.; Malrieu, J.-P. Convergence of an improved CIPSI algorithm. *Chem. Phys.* **1983**, *75*, 91−102.
(23) Cimiraglia, R.; Persico, M. Recent advances in multireference second order perturbation CI: The CIPSI method revisited. *J. Comput. Chem.* **1987**, *8*, 39−47.
(24) Siegbahn, P. E. M.; Almlöf, J.; Heiberg, A.; Roos, B. O. The complete active space SCF (CASSCF) method in a Newton−Raphson formulation with application to the HNO molecule. *J. Chem. Phys.* **1981**, *74*, 2384−2396.
(25) Jorgen, H.; Jensen, A.; Jorgensen, P.; Ågren, A.; Olsen, J. Second-order Møller−Plesset perturbation theory as a configuration and orbital generator in multiconfiguration self-consistent field calculations. *J. Chem. Phys.* **1988**, *88*, 3834−3839.
(26) Hoyer, C. E.; Li Manni, G.; Truhlar, D. G.; Gagliardi, L. Controversial Electronic Structures and Energies of Fe2, Fe2+, and Fe2- Resolved by RASPT2 Calculations. *J. Chem. Phys.* **2014**, *141*, 204309.
(27) Ivanic, J. Direct Configuration interaction and MC-SCF method for multiple active space swith variable occupation. I. Method (ORMAS). *J. Chem. Phys.* **2003**, *119*, 9364−9376.
(28) Cimiraglia, R. Second order perturbation correction to CI energies by use of diagrammatic techniques: An improvement to the CIPSI algorithm. *J. Chem. Phys.* **1985**, *83*, 1746−1749.
(29) Cacelli, I.; Ferretti, A. *QUIOLA: a program for general modification of molecular orbitals*, 1.0; Pisa, 2008.
(30) Davidson, E. R. The iterative calculation of a few of the lowest eigenvalues and corresponding eigenvectors of large real-symmetric matrices. *J. Comput. Phys.* **1975**, *17*, 87−94.
(31) Grimme, S.; Waletzke, M. Multi-reference Møller−Plesset theory: computational strategies for large molecules. *Phys. Chem. Chem. Phys.* **2000**, *2*, 2075−2081.
(32) Musch, P.; Engels, B. DIESEL-MP2: a new program to perform large-scale multireference-MP2 computations. *J. Comput. Chem.* **2006**, *27*, 1055−1062.
(33) Angeli, C.; Cimiraglia, R. Multireference perturbation CI IV. Selection procedures for one-Elecron properties. *Theor. Chem. Acc.* **2001**, *105*, 259−264.
(34) Shamasundar, K. R.; Knizia, G.; Werner, H.-J. A new internally contracted multi-reference configuration interaction method. *J, Chem. Phys.* **2011**, *135*, 054101.
(35) Werner, H.-J.; Knowles, P. J. An efficient internally contracted multiconfiguration-reference CI method. *J. Chem. Phys.* **1989**, *89*, 5803−5814.
(36) Angeli, C.; Cimiraglia, R.; Persico, M.; Toniolo, A. Multi-reference perturbation CI I. Extrapolation procedure with CAS or selected zero-order spaces. *Theor. Chem. Acc.* **1997**, *98*, 57−63.
(37) Spiegelmann, F.; Malrieu, J. P. The use of effective Hamiltonian for the treatment of avoided crossings. II Nearly diabatic potential curves. *J. Phys. B: At. Mol. Phys.* **1984**, *17*, 1259−1280.
(38) Angeli, C.; Cimiraglia, R.; Persico, M. Multireference perturbation CI III. fast evaluation of one-particle density matrix. *Theor. Chem. Acc.* **1998**, *100*, 324−328.
(39) Miralles, J.; Castell, O.; Caballol, R.; Malrieu, J.-P. Specific CI calculation of energy differences: Transition energies and bond energies. *Chem. Phys.* **1993**, *172*, 33−43.
(40) Miralles, J.; Daudey, J. P.; Caballol, R. Variational calculation of small energy differences. The singlet-triplet gap in $[Cu_2Cl_6]^{2-}$. *Chem. Phys. Lett.* **1992**, *198*, 555−562.
(41) Barone, V.; Boilleau, C.; Cacelli, I.; Ferretti, A.; Monti, S.; Prampolini, G. Structure−Properties Relationships in Triplet Ground State Organic Diradicals: A Computational Study. *J. Chem. Theory Comput.* **2013**, *9*, 300−307.
(42) Barone, V.; Boilleau, C.; Cacelli, I.; Ferretti, A.; Prampolini, G. Conformational Effects on the Magnetic Properties of an Organic Diradical: A Computational Study. *J. Chem. Theory Comput.* **2013**, *9*, 1958−1963.
(43) Barone, V.; Cacelli, I.; Cimino, P.; Ferretti, A.; Monti, S.; Prampolini, G. Magnetic interactions in phenyl-bridged nitroxide diradicals: conformational effects by multireference and broken symmetry DFT approaches. *J. Phys. Chem. A* **2009**, *113*, 15150.
(44) Barone, V.; Cacelli, I.; Ferretti, A. Magnetic coupling in bis-nitronylnitroxide radicals: The role of aromatic bridges. *J. Chem. Phys.* **2009**, *130*, 94306.
(45) Barone, V.; Cacelli, I.; Ferretti, A.; Girlanda, M. Toward an effective yet reliable many-body computation of magnetic couplings in bisnitronyl nitroxide biradicals. *J. Chem. Phys.* **2008**, *128*, 174303.
(46) Barone, V.; Cacelli, I.; Ferretti, A.; Monti, S.; Prampolini, G. Singlet-triplet energy gap of a diarylnitroxide diradical by an accurate many-body perturbative approach. *Phys. Chem. Chem. Phys.* **2011**, *13*, 4709−4714.

DOI: 10.1021/ct501071k
J. Chem. Theory Comput. XXXX, XXX, XXX−XXX

(47) Barone, V.; Cacelli, I.; Ferretti, A.; Monti, S.; Prampolini, G. An Integrated Protocol for the Accurate Calculation of Magnetic Interactions in Organic Magnets. *J. Chem. Theory Comput.* **2011**, *7*, 699−706.
(48) Barone, V.; Cacelli, I.; Ferretti, A.; Prampolini, G. Modified virtual orbitals for CI calculations of energy splitting in organic diradicals. *Phys. Chem. Chem. Phys.* **2009**, *11*, 3854−3860.
(49) Barone, V.; Cacelli, I.; Ferretti, A.; Prampolini, G. Accurate yet feasible post-Hartree-Fock computation of magnetic interactions in large biradicals through a combined variational/perturbative approach: Setup and validation. *J. Chem. Phys.* **2009**, *131*, 224103.
(50) Schmidt, M. W.; Baldridge, K. K.; Boats, J. A.; Elbert, S. T.; Gordon, M. S.; Jensen, J. H.; Koseki, S.; Matsunaga, N.; Nguyen, K. A.; Su, S. J.; Windus, T. L.; Dupuis, M.; Montgomery, J. A. General atomic and molecular electronic structure system. *J. Comput. Chem.* **1993**, *14*, 1347−1363.
(51) Calzado, C. J.; Cabrero, J.; Malrieu, J.-P.; Caballol, R. Analysis of the magnetic coupling in binuclear complexes. I. Physics of the coupling. *J. Chem. Phys.* **2002**, *116*, 2728−2747.
(52) Cacelli, I.; Campanile, S.; Denti, G.; Ferretti, A.; Sommovigo, M. $[(NH_3)_5Ru(1,2,4,5\text{-tetrazine})]^{2+}$: Synthesis and Experimental and Theoretical Study of Its Solvatochromism in the Visible Spectral Region. *Inorg. Chem.* **2004**, *43*, 1379−1387.
(53) Cacelli, I.; Ferretti, A. Solvent effect on the optical properties of $(NH_3)_5Ru$-pyrazine^{+m} (m=2,3) complexes by ab initio calculations. *J. Chem. Phys.* **1998**, *109*, 8583−8590.
(54) Cacelli, I.; Ferretti, A. Theoretical study of the absorption spectrum of $(NH_3)_5Ru$-(4,4′-bipyridine)$^{2+}$ in solution. *J. Phys. Chem. A* **1999**, *103*, 4438−4445.
(55) Cacelli, I.; Ferretti, A.; Toniolo, A. Absorption and electroabsorption spectra of $(NH_3)_5Ru(4,4'\text{-bipyridine})Ru(NH_3)_5^{4+}$ in water by ab initio calculations. *J. Phys. Chem. A* **2001**, *105*, 4480−4487.
(56) Angeli, C.; Persico, M. Multireference perturbation CI II: selection of the zero-order space. *Theor. Chem. Acc.* **1997**, *98*, 117−128.
(57) Frisch, M. J. T.; Trucks, G. W.; Schlegel, H. B.; Scuseria, G. E.; Robb, M. A.; Cheeseman, J. R.; Scalmani, G.; Barone, V.; Mennucci, B.; Petersson, G. A.; Nakatsuji, H.; Caricato, M.; Li, X.; Hratchian, H. P.; Izmaylov, A. F.; Bloino, J.; Zheng, G.; Sonnenberg, J. L.; Hada, M.; Ehara, M.; Toyota, K.; Fukuda, R.; Hasegawa, J.; Ishida, M.; Nakajima, T.; Honda, Y.; Kitao, O.; Nakai, H.; Vreven, T.; Montgomery, J. A., Jr.; Peralta, J. E.; Ogliaro, F.; Bearpark, M.; Heyd, J. J.; Brothers, E.; Kudin, K. N.; Staroverov, V. N.; Kobayashi, R.; Normand, J.; Raghavachari, K.; Rendell, A.; Burant, J. C.; Iyengar, S. S.; Tomasi, J.; Cossi, M.; Rega, N.; Millam, N. J.; Klene, M.; Knox, J. E.; Cross, J. B.; Bakken, V.; Adamo, C.; Jaramillo, J.; Gomperts, R.; Stratmann, R. E.; Yazyev, O.; Austin, A. J.; Cammi, R.; Pomelli, C.; Ochterski, J. W.; Martin, R. L.; Morokuma, K.; Zakrzewski, V. G.; Voth, G. A.; Salvador, P.; Dannenberg, J. J.; Dapprich, S.; Daniels, A. D.; Farkas, Ö.; Foresman, J. B.; Ortiz, J. V.; Cioslowski, J.; Fox, D. J. *Gaussian09, Revision D.01*; Gaussian, Inc.: Wallingford, CT, 2009.
(58) Szalay, P. G.; Aquino, A. J. A.; Barbatti, M.; Lischka, H. Theoretical study of the excitation spectrum of azomethane. *Chem. Phys.* **2011**, *380*, 9.
(59) Collier, S. S.; Slater, D. H.; Calvert, J. G. The photochemistry of the azoalkanes. *Photochem. Photobiol.* **1968**, *7*, 737−753.
(60) Robin, M. B.; Hart, R. R.; Kuebler, N. A. Electronic states of the Azoalkanes. *J. Am. Chem. Soc.* **1967**, *89*, 1564−1572.
(61) Biczysko, M.; Bloino, J.; Brancato, G.; Cacelli, I.; Cappelli, C.; Ferretti, A.; Lami, A.; Monti, S.; Pedone, A.; Prampolini, G.; Puzzarini, C.; Santoro, F.; Trani, F.; Villani, G. Integrated computational approaches for spectroscopic studies of molecular systems in the gas phase and in solution: pyrimidine as a test case. *Theor. Chem. Acc.* **2012**, *131*, 1201.
(62) Barone, V.; Cacelli, I.; De Mitri, N.; Licari, D.; Monti, S.; Prampolini, G. Joyce and Ulysses: integrated and user-friendly tools for the parameterization of intramolecular force fields from quantum mechanical data. *Phys. Chem. Chem. Phys.* **2013**, *15*, 3736−3751.
(63) Cacelli, I.; Prampolini, G. Parametrization and Validation of Intramolecular Force Fields Derived from DFT Calculations. *J. Chem. Theory Comput.* **2007**, *3*, 1803−1817.
(64) da Silva, F. F.; Almeida, D.; Martins, G.; Milosavljevic, A. R.; Marinkovic, B. P.; Hoffmann, S. V.; Mason, N. J.; Nunes, Y.; Garcia, G.; Limao-Vieira, P. The electronic states of pyrimidine studied by VUV photoabsorption and electron energy-loss spectroscopy. *Phys. Chem. Chem. Phys.* **2010**, *12*, 6717−6731.
(65) Cacelli, I.; Ferretti, A.; Prampolini, G. Perturbative Multi-Reference Configuration Interaction (CI-MRPT2) Calculations in a Focused Dynamical Approach: a Computational Study of Solvatochromism in Pyrimidine. *J. Phys. Chem. A* **2014**, DOI: 10.1021/jp509877q.
(66) de Visser, S. P.; Filatov, M.; Shaik, S. REKS calculations on ortho-, meta- and para-benzyne. *Phys. Chem. Chem. Phys.* **2000**, *2*, 5046−5048.
(67) Evangelista, F. A.; Allen, W. D.; Schaefer, H. F. Coupling term derivation and general implementation of state-specific multireference coupled cluster theories. *J. Chem. Phys.* **2007**, *127*, 024102.
(68) Kim, H.-J.; Wang, X.; Ma, J.; Cho, J.-H. A density-functional-theory study of biradicals from benzene to hexacene. *Chem. Phys. Lett.* **2011**, *516*, 141−145.
(69) Li, X.; Paldus, J. Force field of para- and metabenzyne diradicals: a multireference coupled-cluster study. *J. Chem. Phys.* **2010**, *132*, 114103.
(70) Cramer, C. J.; Nash, J. J.; Squires, R. R. A reinvestigation of singlet benzyne thermochemistry predicted by CASPT2, coupled-cluster and density functional calculations. *Chem. Phys. Lett.* **1997**, *277*, 311−320.
(71) Jagau, T.-C.; Prochnow, E.; Evangelista, F. A.; Gauss, J. Analytic gradients for Mukherjee's multireference coupled-cluster method using two-configurational self-consistent-field orbitals. *J. Chem. Phys.* **2010**, *132*, 144110.
(72) Koseki, S.; Fujimura, Y.; Hirama, M. Benzannelation Effect on Enediyne Cycloaromatization: An ab Initio Molecular Orbital Study. *J. Phys. Chem. A* **1999**, *103*, 7672−7675.
(73) Kraka, E.; Cremer, D. Ortho-, meta-, and para-benzyne. A comparative CCSD (T) investigation. *Chem. Phys. Lett.* **1993**, *216*, 333−340.
(74) Kraka, E.; Cremer, D. CCSD(T) Investigation of the Bergman Cyclization of Enediyne. Relative Stability of o-, m-, and p-Didehydrobenzene. *J. Am. Chem. Soc.* **1994**, *116*, 4929−4936.
(75) Lindh, R.; Bernhardsson, A.; Schütz, M. Benzyne Thermochemistry: A Benchmark ab Initio Study. *J. Phys. Chem. A* **1999**, *103*, 9913−9920.
(76) Prall, M.; Wittkopp, A.; Schreiner, P. R. Can Fulvenes Form from Enediynes? A Systematic High-Level Computational Study on Parent and Benzannelated Enediyne and Enyne−Allene Cyclizations. *J. Phys. Chem. A* **2001**, *105*, 9265−9274.
(77) Shen, J.; Fang, T.; Hua, W.; Li, S. Spectroscopic constants of single-bond diatomic molecules and singlet-triplet gaps of diradicals by the block-correlated coupled cluster theory. *J. Phys. Chem. A* **2008**, *112*, 4703−4709.
(78) Squires, R. R.; Cramer, C. J. Electronic Interactions in Aryne Biradicals. Ab Initio Calculations of the Structures, Thermochemical Properties, and Singlet−Triplet Splittings of the Didehydronaphthalenes. *J. Phys. Chem. A* **1998**, *102*, 9072−9081.
(79) Wierschke, S. G.; Nash, J. J.; Squires, R. R. A multiconfigurational SCF and correlation-consistent CI study of the structures, stabilities, and singlet-triplet splittings of o-, m-, and p-benzyne. *J. Am. Chem. Soc.* **1993**, *115*, 11958−11967.
(80) Winkler, M.; Sander, W. Matrix Isolation and Electronic Structure of Di- and Tridehydrobenzenes. *Aust. J. Chem.* **2010**, *63*, 1013−1047.
(81) Saito, T.; Thiel, W. Analytical gradients for density functional calculations with approximate spin projection. *J. Phys. Chem. A* **2012**, *116*, 10864−10869.

DOI: 10.1021/ct501071k
J. Chem. Theory Comput. XXXX, XXX, XXX−XXX

(82) Malrieu, J.-P.; Trinquier, G. A recipe for geometry optimization of diradicalar singlet states from broken-symmetry calculations. *J. Phys. Chem. A* **2012**, *116*, 8226−8237.
(83) Sander, W. m-Benzyne and p-Benzyne. *Acc. Chem. Res.* **1999**, *32*, 669−676.
(84) Sato, T.; Niino, H. Benzdiynes and Related Dehydroaromatics. *Aust. J. Chem.* **2010**, *63*, 1048−1060.
(85) Sikorav, S.; Bkouche-Waksman, I.; Kahn, O. Crystal structure and magnetic and EPR properties of bis(μ-azido)tetrakis(4-tert-butylpyridine)dicopper(II) perchlorate: a new copper(II) dinuclear complex with a large stabilization of the ground triplet state. *Inorg. Chem.* **1984**, *23*, 490−495.
(86) Wenthold, P. G. Thermochemical Properties of the Benzynes. *Aust. J. Chem.* **2010**, *63*, 1091−1098.
(87) Wenthold, P. G.; Squires, R. R.; Lineberger, W. C. Ultraviolet Photoelectron Spectroscopy of the o-, m-, and p-Benzyne Negative Ions. Electron Affinities and Singlet−Triplet Splittings for o-, m-, and p-Benzyne. *J. Am. Chem. Soc.* **1998**, *120*, 5279−5290.
(88) Wentrup, C. The Benzyne Story. *Aust. J. Chem.* **2010**, *63*, 979−986.
(89) Kahn, O. *Molecular Magnetism*; VCH: New York, 1993; p 110.
(90) Hay, P. J.; Wadt, W. R. Ab initio effective core potentials for molecular calculations. Potentials for the transition metal atoms Sc to Hg. *J. Chem. Phys.* **1985**, *82*, 270.
(91) Hay, P. J.; Wadt, W. R. Ab initio effective core potentials for molecular calculations. Potentials for main group elements Na to Bi. *J. Chem. Phys.* **1985**, *82*, 284.
(92) Hay, P. J.; Wadt, W. R. Ab initio effective core potentials for molecular calculations. Potentials for K to Au including the outermost core orbitals. *J. Chem. Phys.* **1985**, *82*, 299.
(93) Cabrero, J.; Caballol, R.; Malrieu, J. P. Efficiency of a Controlled Use of Davidson's Correction for the Calculation of Excitation Energies: Vertical Spectrum of Trans-Butadiene. *Mol. Phys.* **2002**, *100*, 919−926.
(94) Kurashige, Y.; Chalupský, J.; Lan, T. N.; Yanai, T. Complete active space second-order perturbation theory with cumulant approximation for extended active-space wavefunction from density matrix renormalization group. *J. Chem. Phys.* **2014**, *141*, 174111.
(95) Kurashige, Y.; Yanai, T. Second-order perturbation theory with a density matrix renormalization group self-consistent field reference function: Theory and application to the study of chromium dimer. *J. Chem. Phys.* **2011**, *135*, 094104.
(96) Yanai, T.; Kurashige, Y.; Mizukami, W.; Chalupsky, J.; Lan, T. N.; Saitow, M. Density Matrix Renormalization Group for ab initio Calculations and Associated Dynamic Correlation Methods: A Review of Theory and Applications. *Int. J. Quantum Chem.* **2014**, *115*, 283−299.

DOI: 10.1021/ct501071k
J. Chem. Theory Comput. XXXX, XXX, XXX−XXX